AD-A207 037 DOCUMENTATION PAGE

Form Approved OMB No. 0704-018

Unclassified	1b RESTRICTIVE MARKINGS
2a SECURITY CLASSIFICATION AUTHORITY	3 DISTRIBUTION/AVAILABILITY OF REPORT Approved for public release, distribution unlimited
2b DECLASSIFICATION/DOWNGRADING SCHEDULE	
4 PERFORMING ORGANIZATION REPORT NUMBER(S)	5 MONITORING ORGANIZATION REPORT NUMBER(S) AFOSR-TR- 89-0463
6a NAME OF PERFORMING ORGANIZATION General Electric Electronics Laboratory	6b OFFICE SYMBOL (If applicable)
6c ADDRESS (City, State, and ZIP Code) Electronics Park Building 3 Syracuse, NY 13221	7a NAME OF MONITORING ORGANIZATION Air Force Office of Scientific Research
8a NAME OF FUNDING/SPONSORING ORGANIZATION Air Force Office of Scientific Research	8b OFFICE SYMBOL (If applicable) NE
8c ADDRESS (City, State, and ZIP Code) Building 410 Bolling Air Force Base, DC 20332-6448	7b ADDRESS (City, State, and ZIP Code) Building 410 Bolling Air Force Base, DC 20332-6448
	9 PROCUREMENT INSTRUMENT IDENTIFICATION NUMBER F49620-88-C-0054
	10 SOURCE OF FUNDING NUMBERS PROGRAM ELEMENT NO: 61102F; PROJECT NO: 2305; TASK NO: C1; WORK UNIT ACCESSION N

11. TITLE (Include Security Classification)

Pseudomorphic InGaAs Materials

12 PERSONAL AUTHOR(S)
J.M. Ballingall, P. Ho, P. Martin, T. Yu

13a. TYPE OF REPORT	13b. TIME COVERED	14. DATE OF REPORT (Year, Month, Day)	15. PAGE COUNT
Annual Technical	FROM Mar. 88 TO Mar. 89	March 31, 1989	

16. SUPPLEMENTARY NOTATION

17. COSATI CODES			18. SUBJECT TERMS (Continue on reverse if necessary and identify by block number)
FIELD	GROUP	SUB-GROUP	Epitaxy, AlGaAs-InGaAs-GaAs, pseudomorphic heterostructures strained layer superlattices, dislocations, photoluminescen Hall effect, electron diffraction

19. ABSTRACT (Continue on reverse if necessary and identify by block number)

The objective of this program is to evaluate the dependence of pseudomorphic $In_xGa_{1-x}As$ quality on epitaxial growth conditions and $In_xGa_{1-x}As$ composition. All of the structures are fabricated by molecular beam epitaxy (MBE). The effects of different growth conditions are being evaluated with a combination of characterization techniques, including Hall effect, photoluminescence, transmission electron microscopy (TEM), and in-situ reflection high energy electron diffraction (RHEED). The electron spatial distribution and energy levels for quantized pseudomorphic structures are calculated self-consistently and compared with experiment. Critical layer thickness is shown to be a function of MBE growth temperature and the interuption of $In_xGa_{1-x}As$ growth with a few monolayers of GaAs is shown to smoooth the $In_xGa_{1-x}As$ surface and provide strain energy relief, substantially extending the critical layer thickness. This new class of strained layer heterostructures which are here named thin strained superlattices (TSSL) extends the practical range of application of the GaAs-$In_xGa_{1-x}As$ system and is anticipated to be generally applicable to other strained layer systems. A publication describing the concept and demonstrating its practicality is tentatively scheduled for the May 22, 1989 issue of Applied Physics Letters. Also, results will be presented at the Electronic Materials Conference June 21-23, 1989 at the Massachusetts Institute of Technology. Indium composition, Aluminum Gallium Arsenide, Gallium Ar

20 DISTRIBUTION/AVAILABILITY OF ABSTRACT	21. ABSTRACT SECURITY CLASSIFICATION
☒ UNCLASSIFIED/UNLIMITED ☐ SAME AS RPT. ☐ DTIC USERS	Unclassified
22a. NAME OF RESPONSIBLE INDIVIDUAL Dr. Gerald Witt	22b. TELEPHONE (Include Area Code) (202) 767-4984 3/
	22c. OFFICE SYMBOL NE

DD Form 1473, JUN 86 — Previous editions are obsolete. — SECURITY CLASSIFICATION OF THIS PAGE

89

DTIC ELECTE 17 APR 1989 S E

PSEUDOMORPHIC $In_xGa_{1-x}As$ MATERIALS

ANNUAL TECHNICAL REPORT

for

AIR FORCE OFFICE of SCIENTIFIC RESEARCH

BOLLING AIR FORCE BASE

WASHINGTON, DC

Contract No. F49620-88-C-0054

For the Period

March 1, 1988 - March 30, 1989

Submitted By:

James M. Ballingall, Principal Investigator
General Electric Electronics Laboratory
P. O. Box 4840
Syracuse, NY 13221

PSEUDOMORPHIC $In_xGa_{1-x}As$ MATERIALS

Annual Technical Report

Table of Contents

I. Introduction and Summary

The objective of this program is to evaluate the dependence of pseudomorphic $In_xGa_{1-x}As$ quality on epitaxial growth conditions and $In_xGa_{1-x}As$ composition. All of the structures are fabricated by molecular beam epitaxy (MBE). The effects of different growth conditions are being evaluated with a combination of characterization techniques.

Three major tasks are being undertaken:

1. A study of the limits of pseudomorphic composition and thickness.
2. An examination of the effects of strain on MBE growth of the pseudomorphic system.
3. Addressing the effects of strain on electron transport and defects.

Substantial progress has been made in each of these tasks during this first year of the contract. This progress has enabled the development of (1) a new class of strained layer heterostructures which we call thin strained superlattices (TSSL), and (2) high electron mobility transistor (HEMT) structures with $x = 0.3$ and $x = 0.35$ $In_xGa_{1-x}As$ single quantum well active layers which on separate device projects at GE are yielding state-of-the-art performance. The TSSL concept extends the practical range of application of the GaAs-$In_xGa_{1-x}As$ system and is anticipated to be generally applicable to other strained layer systems. A publication describing the concept and demonstrating its practicality is tentatively scheduled for the May 22, 1989 issue of Applied Physics Letters (see Section III). Results will also be presented at the Electronic Materials Conference June 21-23, 1989 at the Massachusetts Institute of Technology (see Section IV).

II. Research Progress

A. The Limits of Pseudomorphic Composition and Thickness

The understanding of this area is becoming much more clear than it was a year ago. At that time, there were wide discrepancies in the values of critical layer thickness reported for the GaAs-$In_xGa_{1-x}As$ pseudomorphic system. Epitaxial theory states that there is a critical thickness up to which a strained layer of constant lattice misfit can be grown and still maintain coherency with the underlying substrate. Above the critical thickness, the strain can no longer be accommodated elastically and misfit dislocations are generated. The reasons for the reported discrepancies in

critical layer thickness are now clear, partly due to this work as well as the work of others in this field. Principally there are two reasons. First of all, it is now established that the critical thickness is a function of growth conditions. We have demonstrated that lower substrate temperatures promote larger critical thicknesses. The understanding of this is that the kinetic barriers for misfit dislocation formation require sufficient growth temperatures (or post-growth temperatures) to be overcome. It turns out that relatively small differences in growth temperature (±5%) can make significant differences in the dislocation content of these structures. Secondly, the different measurement techniques employed for detecting misfit dislocation density vary widely in their sensitivity.

In this work we have utilized four techniques for detecting misfit dislocations----in-situ reflection high energy electron diffraction (RHEED), Hall electron mobility, photoluminescence, and transmission electron microscopy (TEM). Perhaps all four could be used quantitatively for assessing dislocation densities, though we have relied only on plan view TEM for quantitative analysis. This has a detection limit of $10^4 cm^{-2}$ several orders of magnitude below the equilibrium misfit dislocation density ($\sim 10^{11} cm^{-2}$) for typical pseudomorphic structures (2% misfit strain) completely strain relieved through misfit dislocaitons. This appears also to be about 2 orders of magnitude below the density at which effects of dislocations would normally be observed by Hall effect or photoluminescence. (An exception to this is photoluminescence microscopy[1] which can detect misfit dislocations to a limit of $\sim 10 cm^{-2}$ because of a large sampling area.)

Figure 1 is a plot of critical layer thickness for several pseudomorphic single quantum well structures grown at GE. The solid line is the Matthews-Blakeslee curve for critical layer thickness (CLT) calculated assuming a "single-kink" failure mechanism, i.e., dislocation propagation along the lower interface of the strained layer, the failure mechanism for single quantum well structures. For reference, the dashed line is the Matthews-Blakeslee curve for CLT assuming a "double-kink" failure mechanism, i.e., dislocation propagation along both interfaces of a strained superlattice. At low substrate temperatures (~480°C) we obtain structures with no detectable dislocations, but with thicknesses substantially above the Matthews-Blakeslee single-kink CLT. However, at higher substrate temperatures (~500-540°C) we see excellent agreement with the single-kink curve. As mentioned previously, this is believed to be due to kinetic barriers to single-kink dislocation formation. Coincidentally, the low substrate temperature CLTs are predicted better with the double-

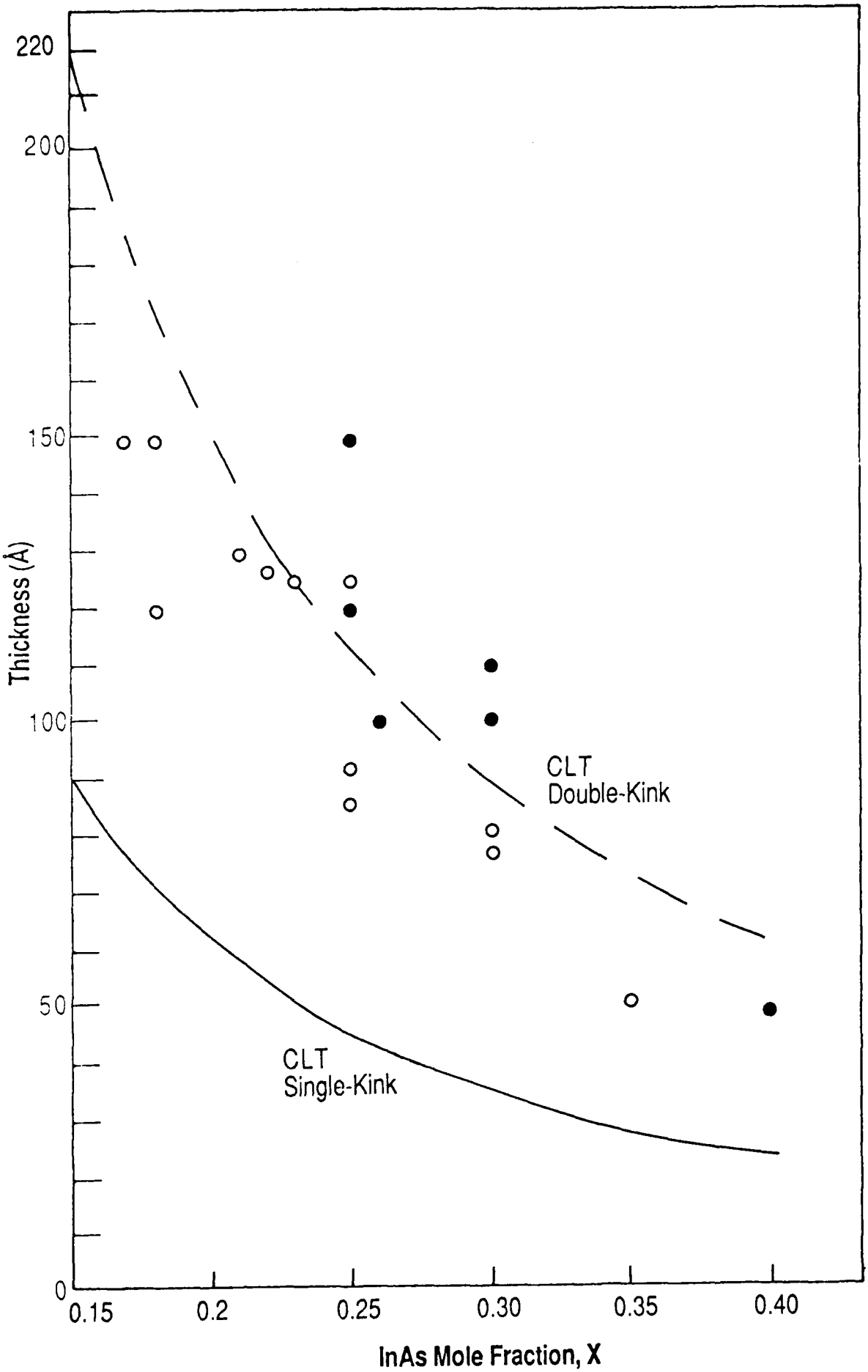

Figure 1.

Critical layer thickness (CLT) for $In_xGa_{1-x}As$ on GaAs according to the Matthews-Blakeslee models for single-kink and double-kink dislocation mechanisms. Plotted points are for modulation-doped single quantum well $AlGaAs-In_xGa_{1-x}As-GaAs$ samples grown at GE by MBE at 480°C. (o-samples with low dislocation densities and acceptable electro-optical properties, ●-samples with high dislocation densities and poor electro-optical properties).

kink curve, at least for $x < 0.3$. The RHEED technique is particularly useful here. Whaley and Cohen[2] demonstrated that the onset of lattice relaxation through misfit dislocations was simultaneously accompanied by three-dimensional growth manifested as spots or chevrons on the RHEED pattern. Their data for $x = 0.33$, some of our previous RHEED data for $x = 0.25$[3], and our RHEED data on this contract for $x = 0.2$ to 0.35 agrees excellently with the Matthews-Blakeslee single-kink curve at the higher substrate temperatures.

By growing at 480°C, we have now been able to demonstrate, on another project, single quantum well $In_{0.3}Ga_{0.7}As$ (70 Å thick) HEMTs with outstanding performance (1.6 dB noise figure with 8.6 dB at 60 GHz). This is not possible with 520°C growth temperatures. Results are expected soon on $x = 0.35$ and $x = 0.4$ single quantum well HEMTs. Thus, the growth technology developed on this contract is already being fruitfully applied to other GE projects which focus on devices.

In addition to the effects of substrate temperature on critical layer thickness, we've discovered in the course of this work that a new structure known as the thin strained superlattice enables the growth of pseudomorphic structures substantially above the critical layer thickness for single quantum wells. As this success is related to surface smoothening of the growth front and strain energy relief, the results are discussed in the next section which deals with the effects of strain on the MBE growth of pseudomorphic structures.

B. The Effects of Strain on MBE Growth of the Pseudomorphic System

The lattice mismatch strain between $In_xGa_{1-x}As$ and GaAs has generally precluded the use of $In_xGa_{1-x}As$ with $x \gtrsim 0.3$ for what are essentially two distinct issues. First of all, the mismatch strain imposes quantum well thicknesses which are too thin for practical devices. The relationship between the $In_xGa_{1-x}As$ critical layer thickness (CLT) and InAs mole fraction x demands that high x pseudomorphic layers have critical thicknesses so thin that quantum size effects push electron subband energy levels up, substantially reducing the electron confinement potential which would be realized with bulk materials or thick quantum wells. Also for thin wells a larger fraction of the electron wave function penetrates more deeply into the AlGaAs barrier layers enhancing the scattering rate. The second issue is that the high x materials, having a lattice mismatch with GaAs greater than 2%, are difficult to grow with high electronic quality. Problems with the crystal growth

manifested as surface roughening, three-dimensional growth, and islanding appear to limit the electronic quality of high x layers[4], even with thicknesses comparable to or less than the CLT.[5]

In this report, we present results for a new class of pseudomorphic HEMT structures which utilizes thin strained superlattice (TSSL) active layers as opposed to the conventional single quantum wells (SQW). These new active layers provide a means for enhancing the InAs mole fraction content of HEMT active layers by simultaneously addressing both of the mismatch strain-related issues mentioned above. A typical TSSL HEMT active layer is shown in Figure 2, with three periods of GaAs(15Å)-$In_{0.3}Ga_{0.7}As$(52Å). The idea is two-fold. First of all, the GaAs layers are sufficiently thin to be relatively transparent to the electrons such that the TSSL contains one two-dimensional electron gas (2-DEG) with a low energy ground state as opposed to three 2-DEGs with considerably higher energy ground states. This enhances the effective conduction band discontinuity compared to a single quantum well or a multi-quantum well with thick GaAs layers. Secondly, the GaAs layers are sufficiently thick to provide strain energy relief and surface smoothening of the $In_xGa_{1-x}As$ to alleviate the problems mentioned above with the crystal growth.

Pseudomorphic HEMT structures were grown by molecular beam epitaxy on LEC GaAs (100) $\pm 0.5°$ oriented substrates. The substrate temperature was 480°C$\pm$10°C for all of the layers with an As_4 to group III beam equivalent pressure ratio of 15 and a nominal growth rate of 1μm/h. The modulation doping was provided by silicon atomic planar-doping at a concentration of $5x10^{12}cm^{-2}$ on top of a 45Å thick undoped $Al_{0.3}Ga_{0.7}As$ spacer layer. 400Å of Si-doped $Al_{0.3}Ga_{0.7}As$ and 350Å of Si-doped GaAs capped the structures as shown in Figure 2. The layers were characterized by Hall effect, photoluminescence, and transmission electron microscopy. All Hall samples were differentially etched to the point of maximizing the measured 77K mobility, in order to minimize the effects of parallel conduction in the doped GaAs and AlGaAs layers. TEM measurements were performed on cross-sectional samples utilizing both bright-field and dark-field imaging modes. Plan view imaging utilized two-beam diffracting conditions in bright-field mode for assessing dislocation densities.

Table 1 shows the effect of layer thickness on electron mobility and sheet density for $In_{0.3}Ga_{0.7}As$ SQWs and GaAs-$In_{0.3}Ga_{0.7}As$ TSSLs. For SQWs the electron mobility is substantially degraded for $x = 0.3$ layers thicker than 80-100Å. Plan-view TEM investigation of the

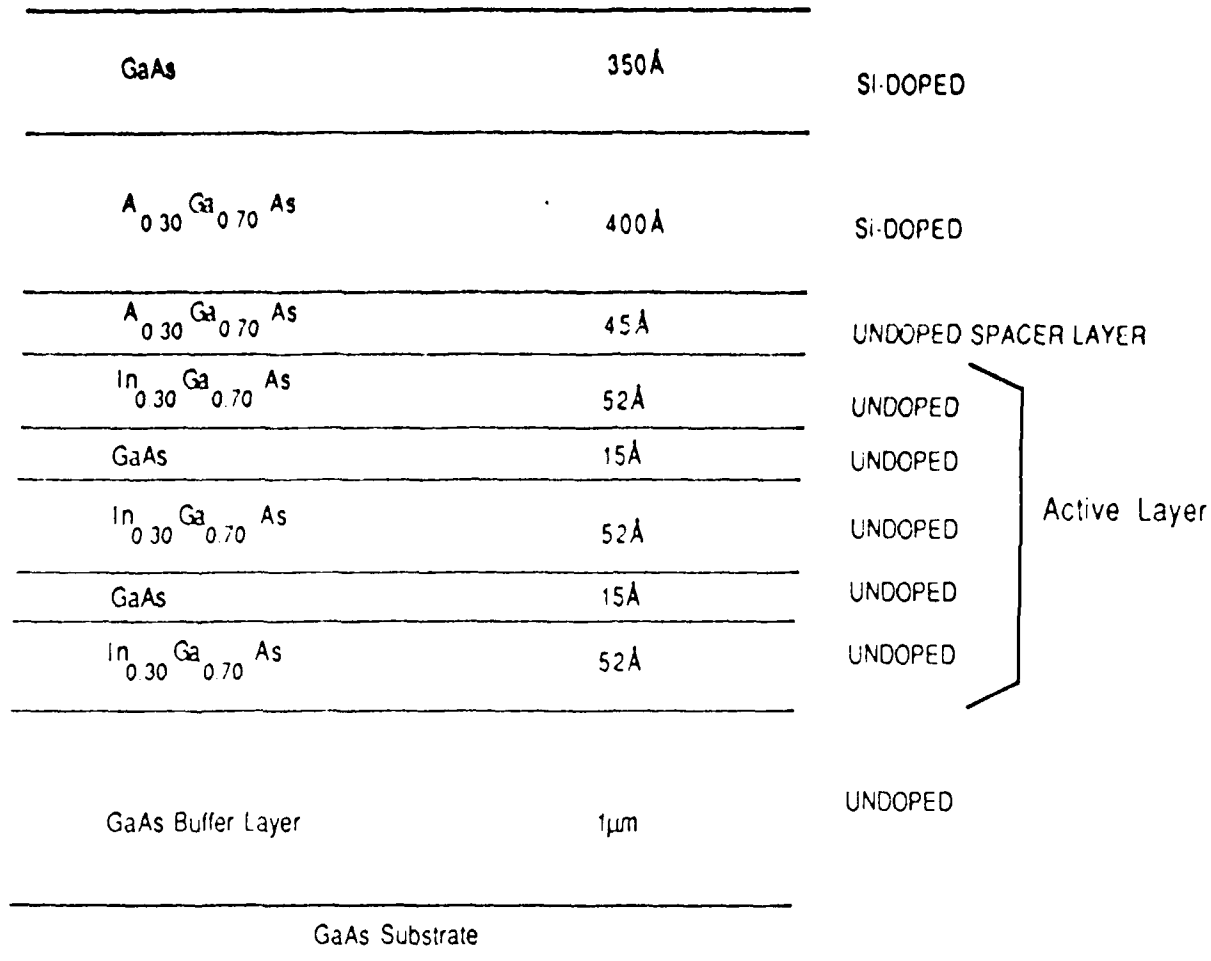

Figure 2.

Schematic cross-section of a modulation-doped pseudomorphic HEMT with a thin strained superlattice (TSSL) active layer.

TABLE 1

ELECTRICAL DATA FOR MODULATION-DOPED PSEUDOMORPHIC STRUCTURES

$In_{0.3}Ga_{0.7}As$ SINGLE QUANTUM WELLS (SQW)

SQW Thickness (Å)	77K Mobility ($cm^2/V\text{-}s$)	77K Sheet Density (cm^{-2})
40	13,800	2.4×10^{12}
80	14,400	2.7×10^{12}
100	700	3.4×10^{12}

$GaAs(h_1)$-$In_{0.3}Ga_{0.7}As(h_2)$ THIN STRAINED SUPERLATTICES (TSSL)

h_1/h_2 (Å)	TSSL Thickness (Å)	77K Mobility($cm^2/V\text{-}s$)	77K Sheet Density (cm^{-2})
15/30	135	12,700	2.5×10^{12}
15/42	171	10,300	2.6×10^{12}
15/52	201	9,200	3.0×10^{12}

100Å thick SQW showed a dislocation density of $10^{10}cm^{-2}$, which is obviously responsible for the dramatic degradation in electron mobility compared to the thinner SQWs. The TSSLs, on the other hand, show a more gradual and less severe degradation in electron mobility; for a total $In_{0.3}Ga_{0.7}As$ thickness of 156Å and a total TSSL thickness of 201Å, the electronic parameters are still quite acceptable.

Figure 3(a) shows a cross-sectional TEM superlattice bright field image of the thickest TSSL listed in Table 1 and shown schematically in Figure 2. Only one misfit dislocation was seen in all of the cross-sectional areas examined, and this dislocation occurred at the interface between the GaAs buffer layer and the first InGaAs layer. Plan-view TEM such as shown in Figure 3(b) confirmed a misfit dislocation density of $10^6/cm^2$ in this sample. Plan-view TEM of the thinner TSSL's detected no dislocations down to a detection limit of $10^4/cm^2$.

Figure 4 shows two plots of critical layer thickness versus strain calculated using the concepts developed recently concerning the stability and metastability for buried strained layers.[6] Critical layer thicknesses are calculated for the "single-kink" failure mechanism, i.e., dislocation propagation along the lower interface of the strained layer, for (1) an uncapped strained layer and (2) a strained layer capped with an 800Å-thick unstrained layer. Good agreement is observed, as mentioned in Section II A, between the uncapped CLT curve of Figure 4 and temperature dependent in-situ reflection high energy electron diffraction (RHEED) measurements when the substrate temperatures are sufficiently high to apparently circumvent kinetic barriers to dislocation formation. These results, in fact, led us to utilize the relatively lower substrate temperature of 480°C for this work. The total thickness of the strained layers of Table 1 is also plotted in Figure 4 versus their strain. To calculate the strain for the TSSLs, we utilized the "free-standing" lattice constant of the TSSL, i.e. we treat the TSSL as if it has an in-plane lattice constant given by the following expression.[7]

$$a = a_1 \left[1 + \frac{(a_2 - a_1)/a_1}{1 + (G_1 h_1 / G_2 h_2)} \right] \qquad (1)$$

where a_1 and a_2 are the lattice constants for GaAs and $In_xGa_{1-x}As$, respectively, h_1 and h_2 are the thicknesses of the GaAs and $In_xGa_{1-x}As$ layers forming each period for the TSSL, and G_1 and G_2

(a)

Figure 3.

(a) Cross-sectional (110) transmission electron micrograph of TSSL shown schematically in Figure 2, demonstrating pseudomorphic growth (superlattice bright field imaging mode).

(b) Plan-view (100) bright field transmission electron micrograph of the above TSSL showing linear misfit dislocations which lie along $< 110 >$. Bend contours (wavy lines) are also visible. Dislocation density in this sample is $10^6/cm^2$. No dislocations were detected in the thinner TSSLs down to a detection limit of $10^4/cm^2$.

(b)

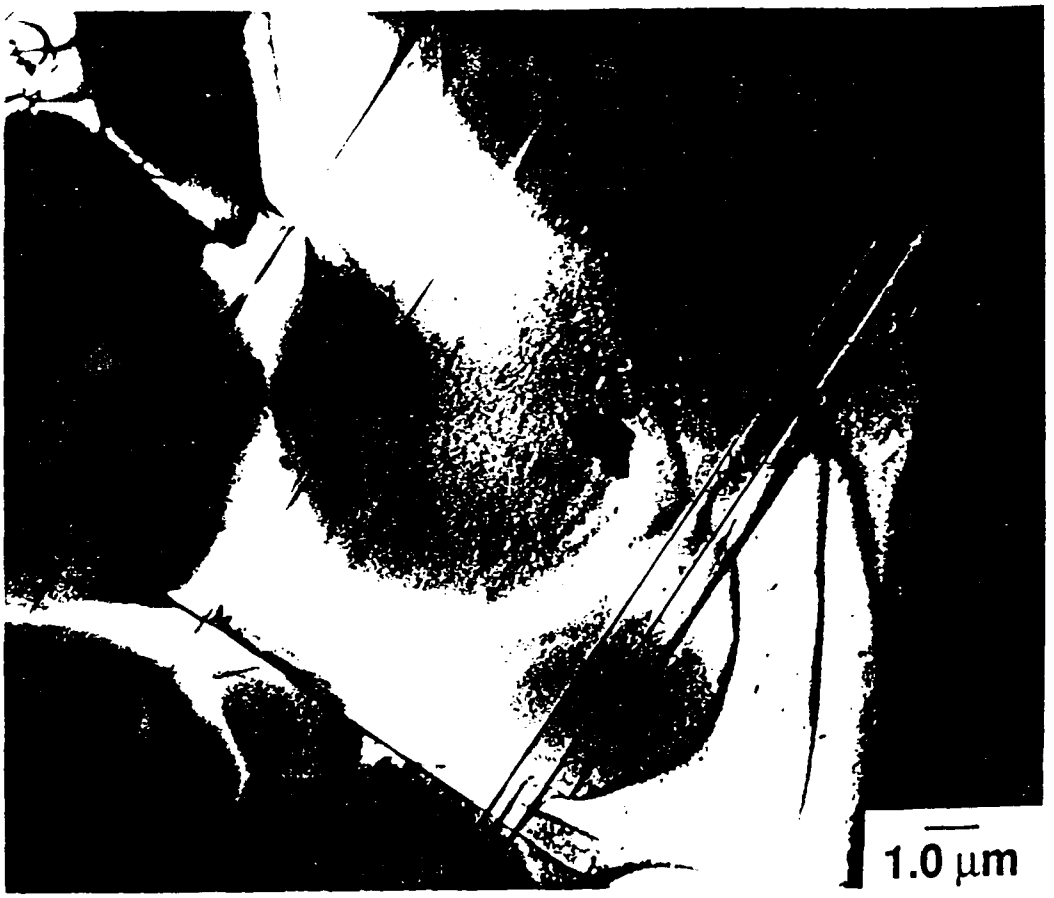

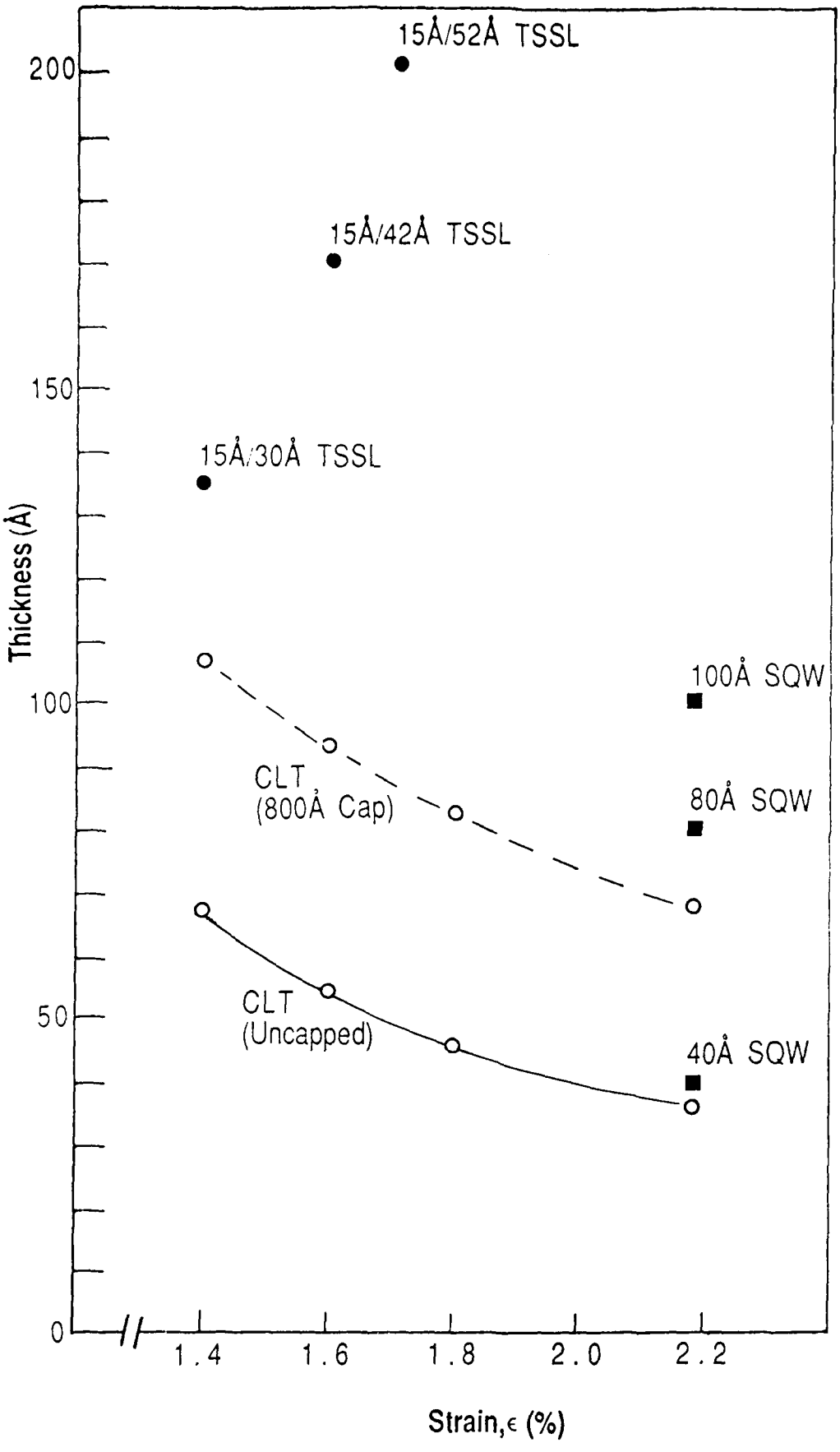

Figure 4.

Plots of layer thickness vs. strain for SQWs and TSSLs listed in Table I. Solid and dashed lines are theoretical critical layer thicknesses (CLT) for, respectively, an uncapped strained layer and a strained layer with an 800Å-thick unstrained capping layer. Both curves assume the single-kink failure mechanism.

are the respective shear moduli for each material (assumed equal for these structures). All of the layers, except for the 40Å SQW, have thicknesses exceeding the CLT for strained layers with an 800Å unstrained capping layer, and so like most psuedomorphic HEMT structures, are predicted to be metastable. Thus, the TSSLs would be expected to degrade with high temperature processing such as post-implant annealling, but otherwise could be expected to be long-lived because of the sluggish kinetics for dislocation formation.[6] It is not clear why the TSSLs can be grown to thicknesses which exceed their respective CLTs more than the SQWs; though strain, being the driving force for dislocation formation and perhaps as well for changes in growth kinetics[8] independent of dislocation formation, is significantly reduced and assumed to be the key factor.

Several authors have reported the continual diminishing of the in-situ RHEED intensity with the growth of pseudomorphic $In_xGa_{1-x}As$[2, 9, 10]. For GaAs-$In_xGa_{1-x}As$-GaAs double heterostructures, it was noted that the decrease in RHEED intensity which occurred during the $In_xGa_{1-x}As$ layer was followed by a substantial recovery in intensity during the GaAs overlayer, an effect which the authors related to three-dimensional growth.[10] We find that the RHEED intensity generally recovers to 70-90% of its starting intensity after only 5 monolayers of GaAs on $In_xGa_{1-x}As$. When the In beam is recommenced for the successive $In_xGa_{1-x}As$ layer, the intensity again diminishes, but then later recovers with the following GaAs layer. Thus, for TSSL growth, the RHEED intensity exhibits periodic oscillations with the superlattice period. Very similar behavior has been reported for GaAs-AlAs short period superlattices and attributed to surface roughening by the AlAs layers alternated with smoothening by the GaAs layers.[11] Contrary to the results quoted above for double heterostructures[10], we did not observe any three-dimensional features (e.g., spots or chevrons) on the RHEED patterns of the TSSLs, and so favor an interpretation here based simply on surface smoothening by the GaAs layers. The lack of three-dimensional features on the RHEED pattern for the TSSLs is in agreement with the temperature dependent RHEED studies cited earlier.[2, 3]

After succeeding with the $x = 0.3$ TSSLs, we began development of $x = 0.35$ and $x = 0.4$ TSSLs. Table 2 lists the structural parameters (composition and thickness) with the Hall mobilities for some of those layers. Three period superlattices for $x = 0.35$ had rather low electron mobilities, so we investigated two period TSSLs for $x = 0.35$ and $x = 0.4$. For both of those values, as the $In_xGa_{1-x}As$

TABLE 2

ELECTRICAL DATA FOR MODULATION-DOPED GaAs(h_1)-$In_xGa_{1-x}As$(h_2) TSSLs

x	h_1/h_2 (Å)	No. of Periods	77K Mobility ($cm^2/V\text{-}s$)	77K Sheet Density (cm^{-2})
0.35	15/30	3	2,500	2.6×10^{12}
0.35	15/32	2	11,800	2.5×10^{12}
0.35	15/40	2	4,100	2.9×10^{12}
0.40	15/25	2	7,800	2.3×10^{12}
0.40	15/34	2	1,100	3.7×10^{12}

layer thickness increases, the mobility degrades, however, both the thinner 0.35 and 0.4 structures look promising for device applications. TEM is in progress on all of these structures, and has been completed on the $x = 0.35$ three period TSSL. Interestingly, while the mobility is low for that sample (2500 $cm^2/V\text{-}s$), TEM showed no misfit dislocations down to a detection limit of 10^4 cm^{-2}. Strain calculated using equation 1 is less than that for $x = 0.3$ single quantum wells so we are led to conclude that the mobility degradation is due to some other mechanism, besides strain or dislocations, perhaps interfacial roughness. Work is continuing in this area to understand this phenomenon.

In summary, results were presented on a novel type of pseudomorphic HEMT structure with a thin strained superlattice (TSSL) active layer. Besides being applied to HEMTs and other transistors, TSSLs are anticipated to extend the wavelength range of pseudomorphic lasers and detectors, as well as possibly enhancing the range of application of other strained materials systems.

C. The Effects of Strain on Electron Transport and Defects

Section II B above included considerable discussion on the effects of strain and dislocations on electron mobility. This section addresses the effects of strain on the photoluminescence (PL) spectra of single quantum well and TSSL pseudomorphic structures. Theoretical modelling of the two-dimensional electron gas spatial distribution and energy levels in these structures are compared with PL spectra.

We have performed low temperature photoluminescence on several of the modulation-doped samples grown for this study. Some results are shown in Table 3. In cases where multiple peaks were observed, the principle peak (largest magnitude) is listed in the table. Figures 5 and 6 show representative spectra. Emission from the single quantum well samples tends to show broader peaks closer to the unstrained InGaAs band gap, while the TSSL peaks are sharper and closer to the predicted transition energies. TSSL spectra show a smaller, broader peak in addition to the sharp quantum well peak recorded in Table 3. The broader peaks have been observed elsewhere and have been attributed to impurity or interface states.[13] In every case, photoluminescence transition energies are substantially below those predicted by the square well model. We expect that the Airy function model, which calculates the effective narrowing of the band gap by the voltage drop across the channel, due to the modulation doping, will give better agreement. Unfortunately, the proper

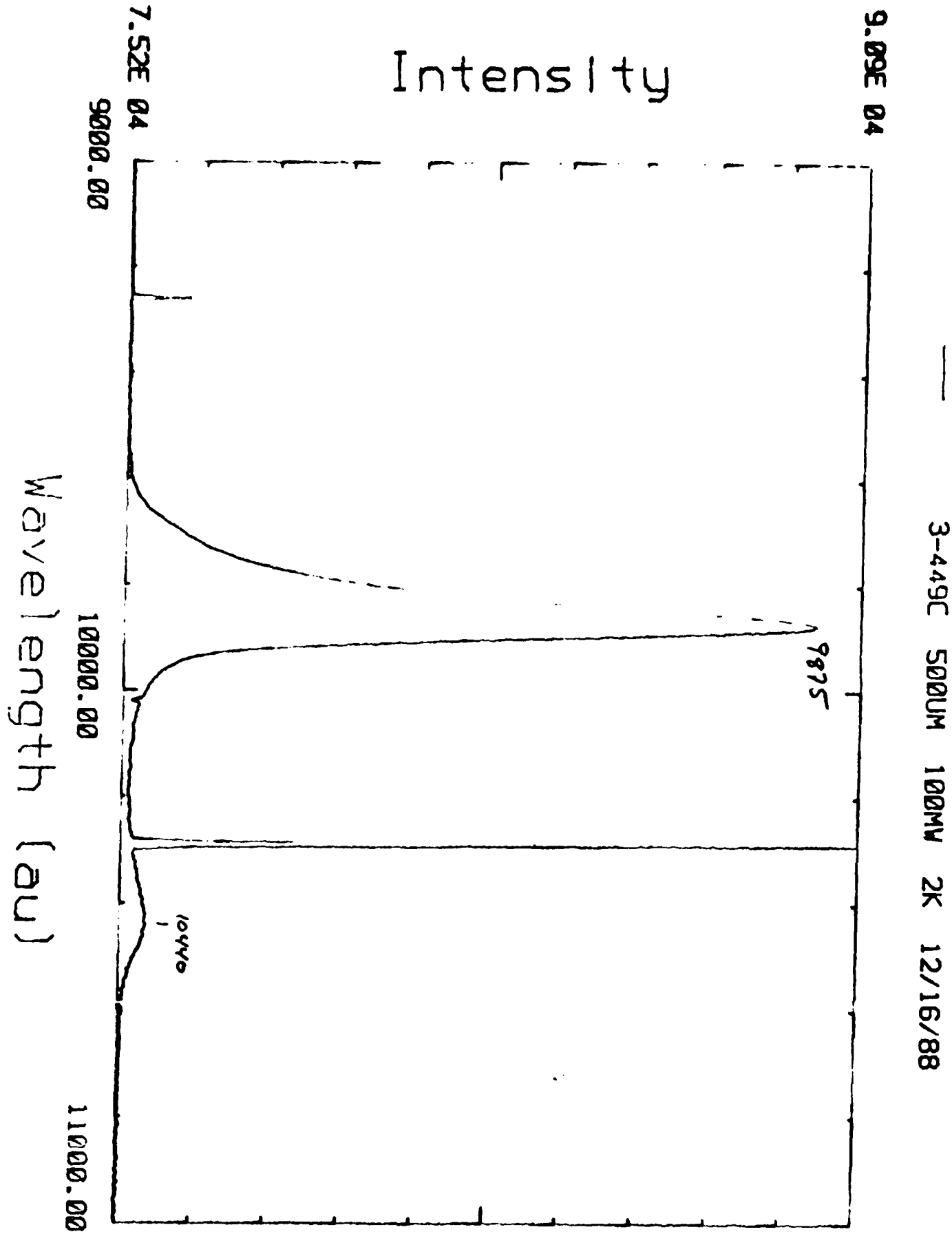

Figure 5.

2K Photoluminescence scan of a modulation-doped pseudomorphic HEMT structure with a TSSL GaAs (15Å)-$In_{0.3}Ga_{0.7}As$ (42Å) three period active layer. The peak at 9875 Å is the n = 1 electron to heavy hole transition. The peak at 10,440Å is attributed to impurities or interface states.

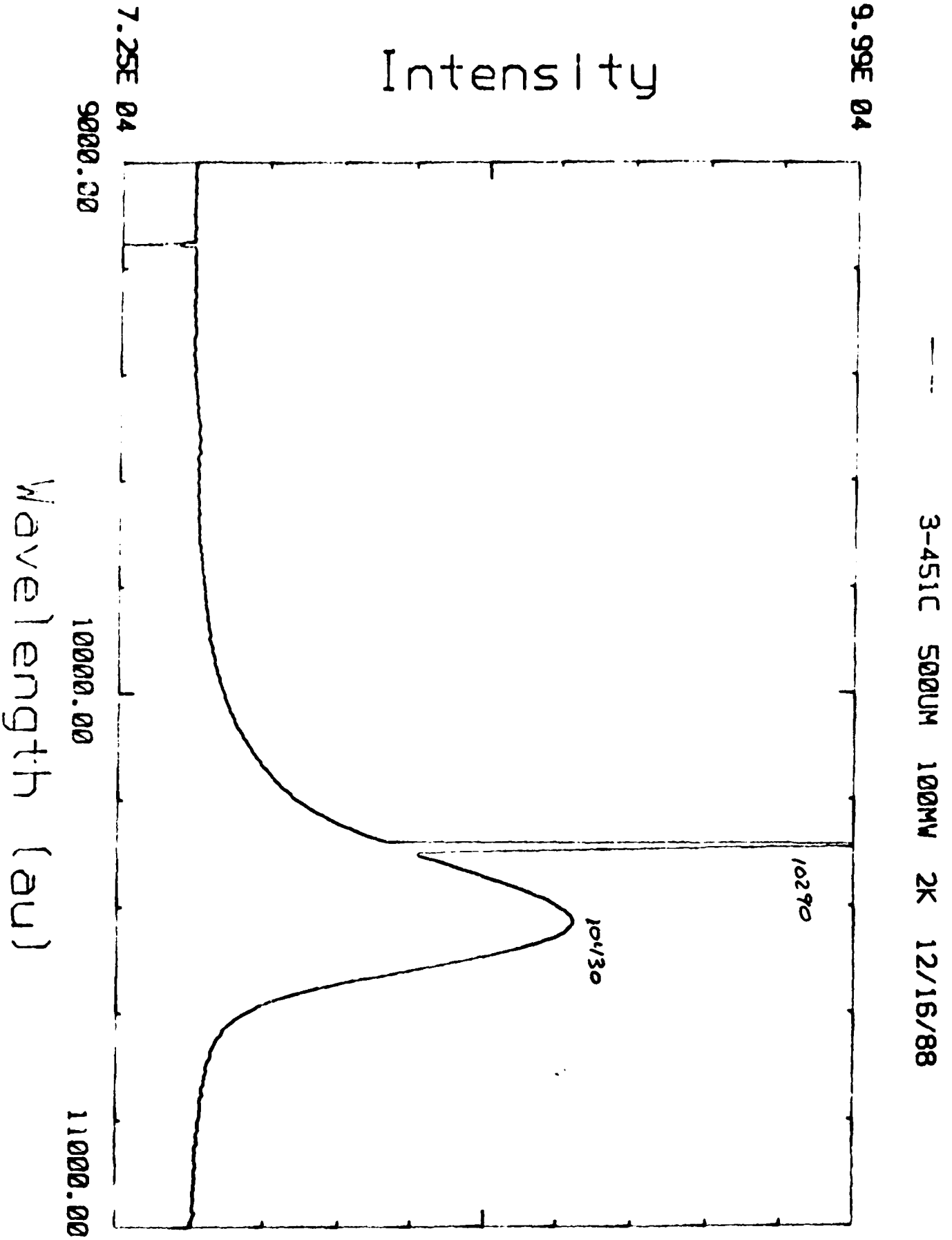

Figure 6.

2K Photoluminescence scan of a modulation-doped pseudomorphic HEMT structure with an $In_{0.3}Ga_{0.7}As$ 78Å-thick single quantum well active layer. The peak at 10,430Å is the n = 1 electron to heavy hole transition.

Table 3

PHOTOLUMINESCENCE RESULTS for GaAs (h_1)-$In_xGa_{1-x}As$(h_2)

TSSLs and $In_xGa_{1-x}As$ SQWs

x	h_1/h_2 (Å)	No. of Periods	Predicted Wavelength (Å)	Observed Wavelength (Å)
0.25	15/30	3	8872.8	not yet done
0.30	15/30	3	9029.6	9348
0.30	15/42	3	9061.6	9875
0.30	15/52	3	9151.9	10055
0.35	15/30	3	9089.8	9900
0.30	15/62	2	9165.5	10170
0.35	15/32	2	8972.1	9712(?)
0.35	15/40	2	9135.2	no peak seen
0.40	15/34	2	9215.0	10060
0.40	15/25	2	8941.8	9460
0.30	78	SQW	9113.5	10430
0.30	80	SQW	9128.9	10490
0.35	50	SQW	9004.7	10500
0.40	48	SQW	9691.7	10860

treatment of the valence bands is incorporated only into the latest version of the model, which is still under development as described below.

The first model developed for this program was a general purpose square well model. This used a transfer matrix approach[14]. This model is capable of arbitrary quantum well structures, and provided the program structure for all subsequent models. The conduction, heavy hole and light hole valence bands are modeled separately within an effective mass approximation. Given the energy levels and the relevant band gaps, the photoluminescence transition energies can be calculated trivially. In accordance with the assumption of zero electric field, the wave functions are made up of sine and cosine functions in the wells and decaying and rising exponentials in the barriers.

The square well model is, of course, not entirely adequate for the structures considered here or a working device structure, since the presence of a Schottky barrier and/or modulated planar doping imposes a considerable electric field on the well. The square well model was therefore modified to construct the wave functions from Airy functions. The Airy function is the exact solution to Schrodinger's equation in a uniform electric field[15]. If we subdivide each layer as necessary into several smaller regions, each of which has a uniform electric field, we can approximate the true potential with one for which the exact wave functions can be found. Given the wave functions and the occupation of the various states, one can calculate the electron distribution in the channel and its contribution to Poisson's equation. We thus solve Schrodinger's and Poisson's equations self-consistently to find the energy levels, occupation and distribution of electrons in the conduction band under operating conditions. Finally, we include in our model the planar doping region (which forms a quantum well in its own right) and the Schottky barrier with applied gate voltage in order to complete the model of the entire structure.

The valence band is modeled in the same way with the exception that no self-consistency is required, as we assume that electrons are the only mobile carriers in the structure present in sufficient quantities to affect Poisson's equation. This assumes low levels of electron-hole pair injection under photoluminescence. To account for the opposite charge of the holes, we reverse the sign of the electric fields to construct the valence band quantum well. Finally, we compute the photoluminescence transition energy by adding the band gap to the sum of the ground state energies, and subtracting the voltage drop across the quantum well. Exciton binding energies are not

calculated or included at this point. We find in general that the field imposed by the planar doping lowers the transition energy due to the effective reduction of the band gap by the voltage drop across the well. This is in spite of the tendency of the field to raise the energy levels in each well.

A sample calculation is shown in Figure 7 for the conduction band of a TSSL structure with three periods of $In_{0.3}Ga_{0.7}As$ (30Å)-GaAs(15Å). The $In_{0.3}Ga_{0.7}As$ layers in this case are divided into two sublayers each to approximate a continuously varying electric field. The square of the wave function is plotted for each of three energy levels. Since the Fermi level nearly coincides with the ground state energy level, the two excited states will have negligible occupation for this room temperature calculation. The model confirms the intuitive result that the TSSL electrons tend to be spatially concentrated in the $In_{0.3}Ga_{0.7}As$ layer closest to the AlGaAs modulation doped layer and have a small probability distribution in the thin GaAs layers of the TSSL.

D. References:

1. P.L. Gourley, I.J. Fritz, and L.R. Dawson, Appl. Phys. Lett., 52, 377 (1988).
2. G.J. Whaley and P.I. Cohen, J. Vac. Sci. Technol. B6, 625 (1988).
3. D.C. Radulescu, W.J. Schaff, L.F. Eastman, J.M. Ballingall, G.O. Ramseyer, and S.D. Hersee, J. Vac. Sci. Technol. B7, 111 (1989).
4. A. Fischer-Colbrie, J.N. Miller, S.S. Laderman, S.J. Rosner, and R. Hull, J. Vac. Sci. Technol. B6, 620 (1988).
5. T. Henderson, M. Aksun, C. Peng, H. Morcoc, P.C. Chao, P.M. Smith, K.H.G. Duh, and L.F. Lester, IEEE Electron Device Lett. EDL-7, 645 (1986).
6. P.S. Peercy, B.W. Dodson, J.Y. Tsao, E.D. Jones, D.R. Myers, T.E. Zipperian, L.R. Dawson, R.M. Biefeld, J.F. Klem, and C.R. Hills, IEEE Elecrron Device Lett. EDL-9, 621 (1988).
7. G.C. Osbourn, J. Vac. Sci. Technol. B1, 379 (1983).
8. S.V. Ghaias and A. Madhukar, Appl. Phys. Lett. 53, 1599 (1988).
9. B.F. Lewis, T.C. Lee, F.J. Grunthaner, A. Madhukar, R. Fernandez, and J. Maserjian, J. Vac. Sci. Technol. B2, 419 (1984).
10. P.R. Berger, K. Chang, P.K. Bhattacharya, and J. Singh, J. Vac. Sci. Technol. B5, 1162 (1987).

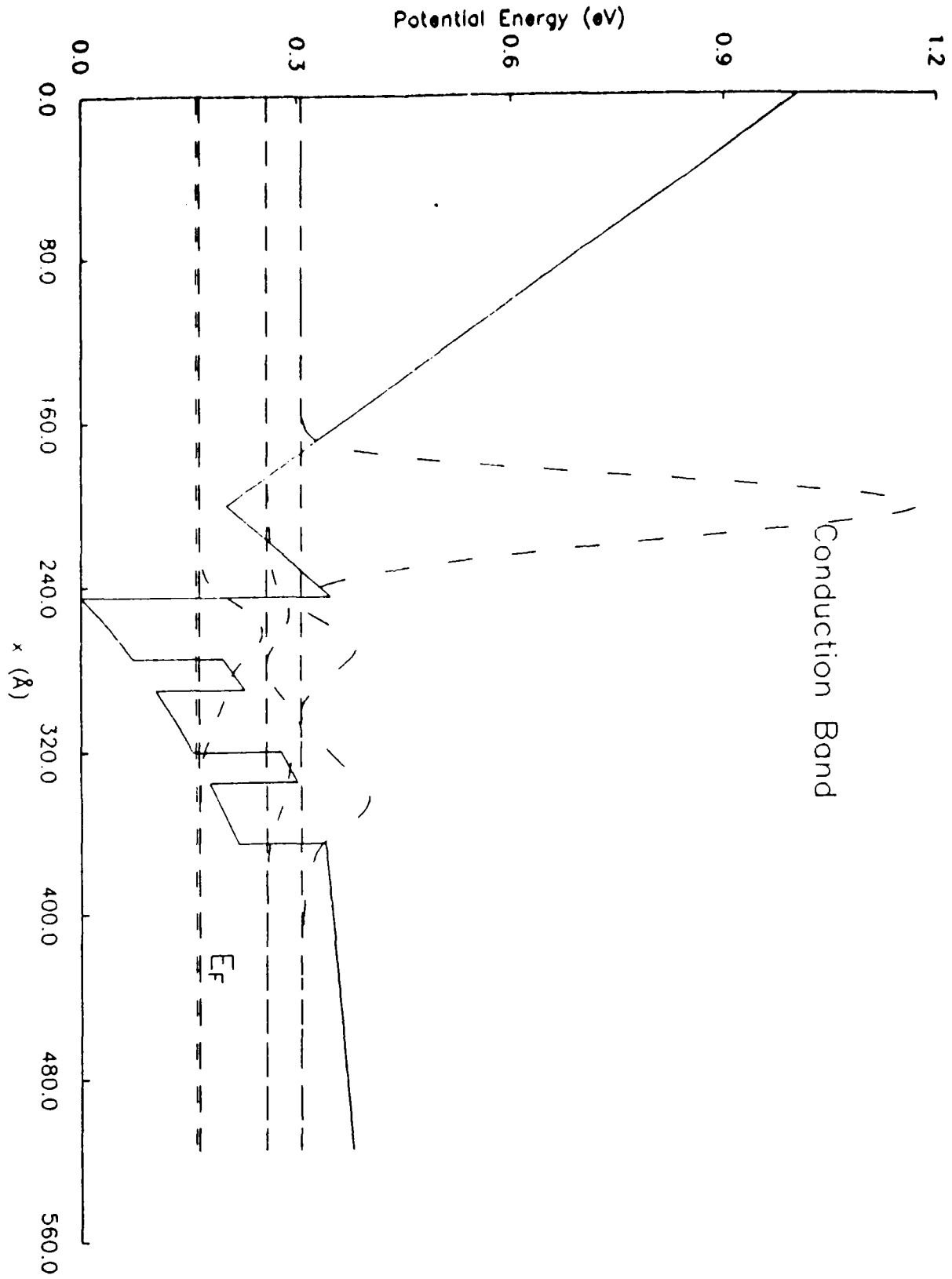

Figure 7.

Electron wave function spatial distribution and energy levels calculated self-consistently from Poisson's and Schrodinger's equations for a modulation-doped (atomic planar doping) HEMT structure with a three period $In_{0.3}Ga_{0.7}As$ (30Å)-GaAs (15Å) TSSL active layer.

11. G.C. Osbourn, J. Vac. Sci. Technol. B1, 379 (1983).

12. J.T. Ebner and J.R. Arthur, J. Vac. Sci. Technol. A5, 2007 (1987).

13. N.G. Anderson, W.D. Ladig, R.M. Kolbas and Y.C. Lo, J. of Appl. Physics 60, 2361 (1980).

14. R. M. Kolbas and N. Holonyak, Jr., Am. J. Phys. 52, 431 (1984)

15. Wayne W. Lui and Masao Fukuma, J. Appl. Phys. 60, 155 (1986), K. F. Brennan and C. J. Summers, J. Appl. Phys. 61, 614 (1987).

III. Publications

The following publication was accepted without revision and is tentatively scheduled for the May 22, 1989 issue of Applied Physics Letters:

"Novel Pseudomorphic High Electron Mobility Transistor Structures with GaAs-$In_{0.3}Ga_{0.7}As$ Thin Strained Superlattice Active Layers," J.M. Ballingall, P. Ho, G.J. Tessmer, P.A. Martin, Nathan Lewis, and Ernest L. Hall.

The following publication is planned for submission this summer to The Journal of Electronic Materials:

"Materials Characteristics of Pseudomorphic High Electron Mobility Transistor Structures with GaAs-$In_xGa_{1-x}As$ ($0.25 < x < 0.4$) Thin Strained Superlattice Active Layers", J.M. Ballingall, P. Ho, P.A. Martin, G.J. Tessmer, T.H. Yu, Nathan Lewis, Ernest Hall.

IV. Interactions

A. The following was accepted for presentation at the 1989 Electronic Materials Conference to be held June 21-23 at the Massachusetts Institute of Technology:

"Materials Characteristics of Pseudomorphic High Electron Mobility Transistor Structures with GaAs-$In_xGa_{1-x}As$ ($0.25 < x < 0.4$) Thin Strained Superlattice Active Layers", J.M. Ballingall, P. Ho, P.A. Martin, G.J. Tessmer, T.H. Yu, Nathan Lewis, Ernest Hall.

B. Several helpful discussions were conducted with Dr. David R. Myers of Sandia National Laboratories concerning his recent work on the stability of pseudomorphic structures (see reference 6 in Section II). These concepts were used for the calculation of CLTs in Figures 1 and 4 of this report.

C. Dr. P.C. Chao of GE is currently fabricating 0.15μm gate length $In_{0.35}Ga_{0.65}As$ single quantum well and TSSL HEMT structures on separate device projects at GE. A 0.15μm $In_{0.3}Ga_{0.7}As$ single quantum well HEMT fabricated at GE yielded outstanding performance at 60 GHz (1.6dB noise figure with 8.6dB gain). Thus, the results of this work are being fruitfully applied to millimeter wave transistor technology.

V. Professional Research Personnel

1. Dr. James M. Ballingall, Principal Investigator
   Manager, Epitaxial Technology
2. Dr. Pin Ho
   Senior Materials Engineer
3. Dr. Tan-hua Yu
   Manager, Materials Characterization
4. Dr. Paul A. Martin
   Materials Engineer
5. Dr. Ernest L. Hall
   Supervisor, Analytical Electron Microscopy
6. Mr. Nathan Lewis
   Materials Engineer
7. Mr. Glenn J. Tessmer
   Materials Engineer